Molecular Pharmacology Fast Forward. Published on December 21, 2007 as doi:10.1124/mol.107.041046
This article has not been copyedited and formatted. The final version may differ from this version.

MOL #41046

Inhibition of Sodium Channel Gating by Trapping the Domain II Voltage Sensor with Protoxin II

Stanislav Sokolov, Richard L. Kraus,* Todd Scheuer, and William A. Catterall

Department of Pharmacology, University of Washington, Seattle, WA 98195-7280

and *Merck Research Laboratories, West Point, PA 19486

Molecular Pharmacology Fast Forward. Published on December 21, 2007 as DOI: 10.1124/mol.107.041046
This article has not been copyedited and formatted. The final version may differ from this version.

Running Title: Voltage Sensor Trapping by Protoxin II

Corresponding author: WILLIAM CATTERALL,
University of Washington School of Medicine Department of Pharmacology
Box 357280, Seattle, WA, United States
Tel: (206) 543-1925, Fax: (206) 543-3882, Email: wcatt@u.washington.edu

Text Pages: 16

Tables: 0

Figures: 8

References: 40

Words in Abstract: 236

Words in Introduction: 726

Words in Discussion: 1256

List of non-standard abbreviations: ProTx-II, protoxin II

Generic name, chemical makeup or citation to published structure of all compounds: None

Color figures: None

Molecular Pharmacology Fast Forward. Published on December 21, 2007 as DOI: 10.1124/mol.107.041046
This article has not been copyedited and formatted. The final version may differ from this version.

Abstract

ProTx-II, an inhibitory cysteine knot toxin from the tarantula *Thrixopelma pruriens*, inhibits voltage-gated sodium channels. Using the cut-open oocyte preparation for electrophysiological recording, we show here that ProTx-II impedes movement of the gating charges of the sodium channel voltage sensors and reduces maximum activation of sodium conductance. At a concentration of 1 μM, the toxin inhibits 65.3 ± 4.1% of the sodium conductance and 24.6 ± 6.8% of the gating current of brain $Na_v1.2a$ channels, with a specific effect on rapidly moving gating charge. The inhibitory effect of ProTx-II can be reversed by strong positive prepulses, indicating voltage-dependent dissociation of the toxin. Voltage-dependent reversal of the ProTx-II effect is more rapid for cardiac $Na_v1.5$ channels, suggesting subtype-specific action of this toxin. Voltage-dependent binding and block of gating current are hallmarks of gating modifier toxins, which act by binding to the extracellular end of the S4 voltage sensors of ion channels. The mutation L833C in the S3-S4 linker in domain II reduces affinity for ProTx-II, and mutation of the outermost two gating-charge-carrying arginine residues in the IIS4 voltage sensor to glutamine abolishes voltage-dependent reversal of toxin action and toxin block of gating current. Our results support a voltage-sensor-trapping model for ProTx-II action in which the bound toxin impedes the normal outward gating movement of the IIS4 transmembrane segment, traps the domain II voltage sensor module in its resting state, and thereby inhibits channel activation.

Molecular Pharmacology Fast Forward. Published on December 21, 2007 as DOI: 10.1124/mol.107.041046
This article has not been copyedited and formatted. The final version may differ from this version.

Introduction

Voltage-gated sodium channels are responsible for the increase in sodium permeability that initiates action potentials in electrically excitable cells and are the molecular targets for several groups of neurotoxins, which bind to different receptor sites and alter voltage-dependent activation, conductance, and inactivation (Catterall, 1980; Cestèle and Catterall, 2000). Sodium channels are composed of one pore-forming α subunit of about 2000 amino acid residues associated with one or two smaller auxiliary subunits, β1 - β4 (Catterall, 2000). The α subunit consists of four homologous domains (I-IV), each containing 6 transmembrane segments (S1-S6), and a reentrant pore loop (P) between S5 and S6 (Catterall, 2000). The S4 transmembrane segments are positively charged and serve as voltage sensors to initiate channel activation (Armstrong, 1981; Catterall, 1986; Stuhmer et al., 1989; Yang and Horn, 1995; Chanda and Bezanilla, 2002). The 'sliding helix' (Catterall, 1986) or 'helical screw' (Guy and Seetharamulu, 1986) models for voltage sensing propose that the S4 segments, which have positively charged amino acids at intervals of three residues, transport gating charge outward to activate sodium channels in response to depolarization by moving along a spiral pathway through the protein structure (Yarov-Yarovoy et al., 2006). This transmembrane movement of the S4 gating segments is a molecular target for neurotoxin action via voltage-sensor trapping (Rogers et al., 1996; Cestèle et al., 1998; Cestèle et al., 2001; Cestèle et al., 2006).

Scorpion venoms contain two groups of polypeptides toxins that alter sodium channel gating. The α-scorpion toxins, as well as sea anemone toxins and some spider toxins, bind to neurotoxin receptor site 3 and slow or block inactivation (Catterall, 1977; Catterall and Beress, 1978; Catterall, 1979; Nicholson et al., 1994). Amino acid residues that contribute to neurotoxin receptor site 3 are localized in the S3-S4 linker in domain IV (Rogers et al., 1996; Benzinger et al., 1998) and in the large extracellular loops in domains I and IV (Tejedor and Catterall, 1988; Thomsen and Catterall, 1989). Binding of toxins to IVS3-S4 is thought to slow inactivation by preventing the normal outward movement of the IVS4 transmembrane segment during channel

Molecular Pharmacology Fast Forward. Published on December 21, 2007 as DOI: 10.1124/mol.107.041046
This article has not been copyedited and formatted. The final version may differ from this version.

gating (Rogers et al., 1996; Sheets et al., 1999). In contrast to these toxins that inhibit inactivation gating, β-scorpion toxins bind to neurotoxin receptor site 4 on sodium channels and enhance activation by shifting its voltage dependence to more negative potentials (Cahalan, 1975; Jover et al., 1980; Jaimovich et al., 1982). Our previous results implicate the extracellular loops S1-S2 and S3-S4 in domain II in formation of neurotoxin receptor site 4. Moreover, a voltage sensor-trapping mechanism, in which the bound β-scorpion toxin holds the IIS4 segment in its outward, activated position was proposed to account for enhancement of activation (Cestèle et al., 2001; Cestèle et al., 2006). Voltage-sensor trapping by both α- and β-scorpion toxins inhibits gating currents generated by the transmembrane movement of the S4 segments, providing a mechanistic signature for voltage-sensor trapping (Nonner, 1979; Meves et al., 1987).

The polypeptide toxins from the tarantula *Thrixopelma pruriens* (Protoxins) are members of the inhibitory cysteine-knot family of protein toxins, consisting of 30 to 35 amino acid residues with three disulfide bridges (Norton and Pallaghy, 1998; Middleton et al., 2002; Priest et al., 2007). This family includes toxins that inhibit activation of sodium channels such as ProTx-II and potassium channels such as hanatoxin by interfering with the normal function of the voltage sensors (Swartz and MacKinnon, 1997; Middleton et al., 2002). Here we have probed the mechanism of ProTx-II action with combined measurements of its effects on sodium currents and gating currents conducted by $Na_V1.2$ and $Na_V1.5$ channels. Our results show that ProTx-II inhibits gating currents conducted during voltage-dependent activation of sodium channels. The inhibitory effects of the toxin can be reversed by strong, long-lasting positive voltage pulses, which drive the voltage sensor into its activated conformation. Voltage-dependent reversal of ProTx-II effects was more rapid for $Na_V1.5$ channels, the primary sodium channel in the heart. Mutations in the S3-S4 linker in domain II reduce toxin affinity, and mutations in the IIS4 voltage sensor prevent voltage-dependent reversal of toxin action. Our results indicate that ProTx-II impedes the normal gating function of the IIS4 voltage sensor by a voltage-sensor trapping mechanism and can be knocked off its receptor site on the extracellular side of the

Molecular Pharmacology Fast Forward. Published on December 21, 2007 as DOI: 10.1124/mol.107.041046
This article has not been copyedited and formatted. The final version may differ from this version.

voltage sensor by voltage-driven movement of the IIS4 voltage sensor into its activated conformation.

Molecular Pharmacology Fast Forward. Published on December 21, 2007 as DOI: 10.1124/mol.107.041046
This article has not been copyedited and formatted. The final version may differ from this version.

Materials and Methods

Materials. ProTx-II from the venom of the tarantula *Thrixopelma pruriens* was synthesized chemically (Middleton et al., 2002). Restriction endonucleases and other molecular biology reagents were purchased from New England Biolabs and Roche Applied Science. Bovine serum albumin (BSA) was from Sigma. pCDM8 vector and the MC1061 *Escherichia coli* bacterial strain were from Invitrogen. cDNAs encoding rat $Na_v1.2a$ α-subunit (Auld et al., 1990) and rat $Na_v1.5$ α-subunit subcloned into pCDM8 vector (Rogers et al., 1996) were used for expression in *Xenopus* oocytes. Point mutations L833C, L833N, E837Q, L838C, L840C, N842A and G845N in the D2S3-S4 linker as well as R850Q, R853Q and a double mutation RR850,853QQ in D2S4 of $Na_v1.2a$ channel were produced in our lab previously (Sokolov et al., 2005). *Xenopus laevis* were purchased from Nasco.

Expression in *Xenopus* oocytes. pCDM8 plasmids encoding rat $Na_v1.5$, $Na_v1.2a$, and mutant $Na_v1.2a$ sodium channel subunits were linearized with XbaI or ClaI respectively, and plasmids encoding β1 subunits were linearized with HindIII. Transcription was performed with T7 RNA polymerase (Ambion Inc., Austin, TX). Isolation, preparation, and maintenance of *Xenopus* oocytes were carried out as described previously (McPhee et al., 1995). Healthy stage V-VI oocytes selected manually were pressure-injected with 50 nl of a solution containing a 1:1 molar ratio of α to β1 subunit RNA. Electrophysiological recordings were carried out 4-7 days after injection.

Cut-open oocyte voltage clamp. Cut-open oocyte voltage-clamp experiments were performed as described by Stefani and Bezanilla (1998) except that access to the cytoplasm was obtained by rupturing the vegetal pole membrane of the oocyte. The oocyte capacitative transients were partially compensated with the voltage clamp amplifier (CA-1; Dagan Corporation). Online P/-4 leak subtraction was used. Microelectrodes were pulled from

Molecular Pharmacology Fast Forward. Published on December 21, 2007 as DOI: 10.1124/mol.107.041046
This article has not been copyedited and formatted. The final version may differ from this version.

borosilicate glass capillary tubes 1.5mm OD (A-M Systems, Carlsborg, WA) and had resistances of 250-350 kΩ when filled with 3M KCl. Extracellular solution contained 120 mM Na-methanesulfonate (MES), 10 mM HEPES, 1.8 mM Ca-MES and 1% BSA, pH=7.4. Internal solution consisted of 110 mM K-MES, 10 mM Na-MES, 10 mM EGTA and 10 mM HEPES, pH=7.4. ProTx-II was prepared as a 100 μM stock in 120 mM Na-methanesulfonate (MES), 10 mM HEPES and 0.2 mg/ml bovine serum albumin, aliquoted at 5 μM, and stored at -20 ˚C. Aliquots containing toxin were thawed immediately prior to experiments and diluted in extracellular solution.

The starting solution volume in the upper boat of the recording chamber (Dagan Corporation) was typically 150 μl. Volumes of 37.5 μl or 50 μl of solution containing 5 μM ProTx-II were typically added to the recording chamber resulting in final concentration of 1 μM to 1.25 μM, except where other concentrations are noted in the Figure Legends, and the cells were allowed to equilibrate for 3 to 5 min before recording. After each experiment the recording and guard chambers were rigorously washed to remove all traces of ProTx-II in a multi-step washing procedure using 75% EtOH and 95% MeOH.

All experiments were performed at room temperature. Currents were filtered at 5 kHz with a low-pass Bessel filter, and then digitized at 20 kHz. Voltage commands were generated using Pulse 8.5 software (HEKA) and ITC- analog to digital interface (Instrutech, Port Washington, N.Y).

Data analysis. Data were analyzed with Igor Pro 4.0 (WaveMetrics). Voltage-clamp protocols are described in the figure legends. Voltage dependences of activation and inactivation were fit by Boltzmann functions of the form $G_{max}/\{1+\exp[(V-V_a)/k]\}$, where G_{max} is the maximum conductance, V_a is the half activation or inactivation potential and k is a slope factor. Rates of inactivation in Fig. 1C were determined by single exponential fitting of current traces. Pooled data are reported as means ± S.E. Statistical comparisons were performed using Student's *t* test, with $p < 0.05$ as the criterion for significance.

Molecular Pharmacology Fast Forward. Published on December 21, 2007 as DOI: 10.1124/mol.107.041046
This article has not been copyedited and formatted. The final version may differ from this version.

Results

Inhibition of sodium currents by ProTx-II. We expressed brain $Na_v1.2a$ channels in *Xenopus* oocytes together with the auxiliary β1 subunits and studied effects of ProTx-II on ionic currents and gating currents with the cut-open voltage clamp technique (Stefani and Bezanilla, 1998). Ionic currents were recorded in 120 mM Na^+ control solution before and 5 min after adding 1 μM ProTx-II to the recording chamber (Fig. 1). ProTx-II (1 μM) inhibited 65.3±4.1% of ionic current in $Na_v1.2$ channels at a test pulse potential of -10 mV (Fig. 1A). Previous results (Middleton et al., 2002) show that the effect of ProTx-II as a function of concentration can be fit by a single binding site model. Plotting the effect of ProTx-II on sodium current versus concentration yielded an inhibition curve that was fit by a single binding site model with EC50 of 540 nM and inhibition of essentially 100% of the sodium current at saturation (Fig. 1B). The EC50 of ProTx-II for sodium channels expressed in Xenopus oocytes is significantly higher than previously observed in mammalian cells (Middleton et al., 2002)

Depolarization to a range of membrane potentials revealed that ProTx-II inhibits activation of sodium channels across the full range of test potentials with little change in the voltage-dependence of activation (Fig. 1C). This is the behavior expected for a toxin that traps a voltage sensor in its resting conformation if sodium channels with toxin bound do not activate during the test pulse, because in this case only unbound channels can activate. Consistent with the evidence that sodium channels with ProTx-II bound do not activate, there were no detectable effects on fast inactivation in the presence of ProTx-II. The rate of entry into the inactivated state (Fig. 1D), the rate of recovery from inactivation (Fig. 1E), and the voltage dependence of fast inactivation (Fig. 1F) were all unaffected by ProTx-II.

Effects of ProTx-II on gating currents. Gating currents of $Na_v1.2a$ channels were recorded in the presence of 1 μM TTX to block ionic conductance through the central pore of the channel. Families of Q_{on} and Q_{off} gating currents were recorded in control solution and after 1 μM ProTx-

Molecular Pharmacology Fast Forward. Published on December 21, 2007 as DOI: 10.1124/mol.107.041046
This article has not been copyedited and formatted. The final version may differ from this version.

II was applied (Fig. 2). ProTx-II substantially reduced the amplitude of gating currents (Fig. 2A). Integration of Q_{on} currents revealed the voltage dependence of gating charge movement across the membrane during sodium channel activation (Fig. 2B). ProTx-II inhibited the gating charge movement across a wide range of membrane potentials. Inhibition of gating charge movement was 24.6 ± 6.4% at +100 mV, the most positive membrane potential studied. On average, 65% reduction of sodium current is caused by 24.6% reduction in gating current (Fig. 2C). By extrapolation assuming the same concentration-response relationship for gating and ionic current (Fig. 1B), a concentration of ProTx-II that inhibits 100% of sodium channels would block 38% of gating charge movement. Evidently, ProTx-II blocks an essential component of gating charge movement, which greatly reduces activation of $Na_V1.2$ channels.

To further define the component of gating charge movement that is blocked by ProTx-II, we measured the kinetics of movement of the Q_{on} gating charge by recording gating currents at high resolution in the absence and presence of 1 μM ProTx-II (Fig. 3A). We found that the toxin blocked only the fast component of Q_{on} movement (Fig. 3B). The shaded area represents the difference between Q_{on} in control and in the presence of toxin. Mean peak Q_{on} current was reduced by 42% at +50 mV, but no significant reduction was observed in Q_{on} current measured late in the pulse when only 20% of the peak Q_{on} current remained (Fig. 3A). Preferential block of the rapid component of Q_{on} current was observed cross a broad range of potentials (Fig. 3C), consistent with the conclusion that the voltage sensor(s) affected by ProTx-II remain the same at all test voltages.

Voltage-dependent reversal of ProTx-II inhibition. Binding of α-scorpion toxins is reversed by strong depolarization, indicating that voltage sensor activation can reverse toxin binding (Catterall, 1977; Rogers et al., 1996). We investigated whether the effects of ProTx-II on ionic currents and gating currents are also reversed by strong depolarization. In the first type of experiment, a strong conditioning depolarization (+100 mV) of increasing duration was followed by 20 ms at the holding potential (-100 mV) to allow recovery from fast inactivation and then by

Molecular Pharmacology Fast Forward. Published on December 21, 2007 as DOI: 10.1124/mol.107.041046
This article has not been copyedited and formatted. The final version may differ from this version.

a test pulse to either –10 mV to measure ionic currents or +50 mV to measure gating currents (Fig. 4). The conditioning pulses reversed ProTx-II inhibition of both ionic and gating currents (Fig. 4B). The amplitudes of both ionic currents and gating currents increased as a result of the depolarizing pulses, and reversal of ProTx-II inhibition followed an exponential time course with similar kinetics for both ionic and gating currents (Fig. 4C). However, even the strongest conditioning depolarizations gave incomplete relief of inhibition of ionic current, reaching 60% to 65% of control at +100 mV and 630 ms.

Applying conditioning pulses of different magnitude ranging from +40 mV to +100 mV allowed us to measure the kinetics of reversal of protoxin inhibition at these voltages (Fig. 5). Reversal of ProTx-II inhibition was fastest and most prominent at +100 mV (τ_{+100mV} = 260 ms, 130% maximum increase in ionic current amplitude) and was very slow at +40 mV (τ_{+40mV} = 1.5 s, 25% maximum increase in amplitude). These results indicate that strong depolarizations are required to overcome the energy of ProTx-II interaction with the resting state of the voltage sensor, drive it into the activated conformation, and cause dissociation of ProTx-II.

The energy required to cause dissociation of the toxin at positive potentials, and thereby permit activation of the channel, shifts the effective activation curve toward more positive potentials for toxin-bound channels, as observed in the voltage dependence of recovery of the sodium current during long depolarizations in the presence of toxin. Plotting the normalized percent increase in test pulse current after 630-ms conditioning depolarizations from the experiments of Fig. 5B versus the conditioning pulse potential results in an isochronal activation curve for toxin-bound channels, which is strongly shifted towards more positive potentials relative to activation of toxin-free channels (Fig. 5C). After a 630-ms conditioning depolarization to +20 mV there is no relief of toxin block, suggesting that toxin-bound channels cannot activate at this potential. Conversely, after 630 ms at +100 mV the current increases 2.33-fold. Further relief is not achieved with increased depolarization. Thus, toxin-bound channels can undergo voltage-dependent activation, but that activation is greatly slowed and positively-shifted due to the energy required to dissociate the toxin from the channel before it can activate.

Molecular Pharmacology Fast Forward. Published on December 21, 2007 as DOI: 10.1124/mol.107.041046
This article has not been copyedited and formatted. The final version may differ from this version.

Protoxin action on cardiac $Na_V1.5$ channels. ProTx-II inhibits sodium currents conducted by $Na_V1.5$ channels to a similar extent as $Na_V1.2$ channels (Middleton et al., 2002; Fig. 6A). However, the reversal of inhibition during strong depolarizations is faster than for $Na_V1.2$ channels (Fig. 6B). This difference in the rate of reversal of ProTx-II inhibition is observed across a wide range of prepulse potentials (Fig. 6C). These results indicate that the dissociation rate for ProTx-II from the activated state of $Na_V1.5$ channels is approximately 2.5-fold faster than for $Na_V1.2$ channels, suggesting subtype-specific effects of ProTx-II on sodium channel gating.

Role of the IIS4 voltage sensor in protoxin binding and action. Our findings that ProTx-II prevents a portion of gating charge movement and that its inhibition of sodium channels is reversed by positive prepulses suggest that ProTx-II is a gating modifier toxin that prevents channel activation via a voltage sensor-trapping mechanism. Previous studies and our results presented so far are most consistent with ProTx-II selectively inhibiting movement of one of the four voltage sensors of sodium channels. Inhibition of sodium currents by ProTx-II is fit by a single binding isotherm, suggesting interaction with a single site (Fig. 1B; Middleton et al., 2002). A rapidly moving component of gating current is selectively inhibited (Fig. 3), suggesting that a kinetically distinct voltage sensor movement is blocked. As the voltage sensor in domain IV moves slowly (Chanda and Bezanilla, 2002), primarily the voltage sensors in domains I, II, and III contribute to the measured gating charge movement. Only 38% of gating charge movement is blocked when channel activation is completely inhibited, consistent with complete inhibition of movement of one of the voltage sensors in domains I, II, or III by ProTx-II. Gating modifier toxins bind to the S3-S4 linkers of sodium channels (Rogers et al., 1996). The β-scorpion toxin Css-IV binds to IIS3-S4 (Cestèle et al., 1998), whereas the α-scorpion toxin LqTx binds to IVS3-S4 (Rogers et al., 1996). Even though ProTx-II stabilizes sodium channels in their closed state and β-scorpion toxins stabilize sodium channels in their open state, they both affect

Molecular Pharmacology Fast Forward. Published on December 21, 2007 as DOI: 10.1124/mol.107.041046
This article has not been copyedited and formatted. The final version may differ from this version.

channel activation via a voltage-sensor trapping mechanism. Since β-scorpion toxins bind to IIS3-S4, we investigated this region as a potential receptor site for ProTx-II.

We analyzed the effects of ProTx-II on mutant $Na_V1.2$ channels with substitutions for selected amino acid residues in the IIS3-S4 loop (Fig. 7). Mutant L833C was significantly resistant to ProTx-II inhibition (27±7% block compared to 65±4% for wild-type, $p<0.05$), suggesting that this amino acid residue may be involved in protoxin binding. The voltage-dependence of activation of L833C mutant channels was similar to that of WT channels (WT: $V_{1/2}$= -26.7 mV; L833C: $V_{1/2}$= -23.8, n=12). Surprisingly, the L833C mutation was quite specific since mutating the same amino acid to N in L833N had no effect on ProTx-II action. In contrast, mutations of the other amino acid residues in the IIS3-S4 loop had lesser or no effect.

If ProTx-II modifies voltage-dependent conformational changes by binding to the outer end of the IIS4 voltage sensor, neutralizing the gating charges in the outer end of the IIS4 segment may affect the toxin-channel interaction considerably. Therefore, we tested whether the double mutant RR850,853QQ, in which the two outer gating charges in IIS4 are neutralized, interacts differently with ProTx-II. Previous studies have shown that these mutations do not substantially alter activation and inactivation of sodium channels (Cestèle et al., 2001; Sokolov et al., 2005). Sodium currents conducted by the double mutant RR850,853QQ were almost as sensitive to 1.25 μM ProTx-II as wild type $Na_v1.2$ channels (Fig. 8A; mean values: 44 ± 5.7%, n = 8 for RR850,853QQ vs 63 ± 5.7%, n=7 for WT). These results indicate that there was no marked reduction in the affinity of the toxin for the resting channel and that the toxin is still able to trap the mutant IIS4 voltage sensor in its resting state.

In contrast to the lack of major effects of these mutations on the function of $Na_V1.2$ channels and the inhibition of ionic current by ProTx-II, the block of gating current by ProTx-II was nearly completely lost in the RR850,853QQ mutant (Fig. 8B). Moreover, voltage-dependent reversal of inhibition during conditioning depolarizations was almost completely abolished in the double mutant RR850,853QQ channel (Fig. 8C, D). No significant voltage-dependent reversal of inhibition was detected for RR850,853QQ with conditioning depolarizations as strong as +150

Molecular Pharmacology Fast Forward. Published on December 21, 2007 as DOI: 10.1124/mol.107.041046
This article has not been copyedited and formatted. The final version may differ from this version.

mV (data not shown). These results indicate that the gating movement of R850 and R853 at the outer end of the IIS4 segment is responsible for voltage-dependent reversal of protoxin inhibition and support the conclusion that ProTx-II interacts specifically with the IIS4 voltage sensor to inhibit gating current.

Molecular Pharmacology Fast Forward. Published on December 21, 2007 as DOI: 10.1124/mol.107.041046
This article has not been copyedited and formatted. The final version may differ from this version.

Discussion

Protoxin blocks gating currents. A signature of gating modifier toxins acting on sodium channels is block of gating charge movement (Nonner, 1979; Meves et al., 1987). This effect likely reflects binding to a specific conformation of the voltage sensor and stabilizing that conformation according to a voltage-sensor trapping mechanism (Rogers et al., 1996; Cestèle et al., 2001; Cestèle et al., 2006). Our results show that ProTx-II shares this signature effect with other gating modifier toxins. By binding to a single site, ProTx-II reduces ON gating charge movement by 24.6 ± 6.4% at 1 μM and by approximately 38% when extrapolated to saturation. The toxin specifically reduces a rapidly moving component of gating charge, suggesting that it selectively impairs the movement of one or more voltage sensors that contribute to the rapid component of gating charge movement.

Voltage-dependent reversal of ProTx-II action. A second hallmark of gating modifier toxins is voltage-dependent enhancement or reversal of toxin action, first demonstrated for reversal of the binding and action of α-scorpion toxins (Catterall, 1977; Rogers et al., 1996). This effect is thought to represent the voltage-driven outward movement of the IVS4 voltage sensor pushing the bound toxin off its binding site. As for α-scorpion toxins, our results show that reversal of ProTx-II action is dramatically accelerated by strong positive prepulses. These results are most consistent with a voltage-sensor trapping model in which ProTx-II binds to one of the four S4 voltage sensors in its resting conformation and holds it in this inward position. Strong positive prepulses provide sufficient electrical energy to force outward movement of the voltage sensor into its activated conformation and are able to overcome the chemical energy of ProTx-II binding and push it off its receptor site. We observe this effect as depolarization-dependent reversal of toxin action.

Molecular Pharmacology Fast Forward. Published on December 21, 2007 as DOI: 10.1124/mol.107.041046
This article has not been copyedited and formatted. The final version may differ from this version.

Protoxin acts on the IIS4 voltage sensor. ProTx-II inhibits sodium channels with a concentration dependence that is fit by a single binding site model (Middleton et al., 2002; Fig. 1B). Because the voltage sensor in domain IV moves slowly (Chanda and Bezanilla, 2002), the voltage sensors in domains I, II, and III likely are primarily responsible for the gating charge movement measured in our experiments. Our findings suggest that approximately 38% of gating current would be blocked by ProTx-II at toxin concentrations where all sodium channels are inhibited. They also show that a rapidly activating component of gating current is preferentially blocked. These results are consistent with the hypothesis that binding of a single ProTx-II molecule inhibits the function of a single voltage sensor.

Three independent lines of investigation implicate the IIS4 voltage sensor in ProTx-II action. First, we found that the mutation L833C in the IIS3-S4 linker reduces the affinity for ProTx-II action, consistent with involvement of this amino acid residue in toxin binding. Second, we found that neutralization of the first two gating-charge-carrying arginine residues in IIS4, R850 and R853, completely prevents the effects of ProTx-II on gating current, indicating that these residues are required for the charge movement blocked by ProTx-II. Neutralization of these gating charges may inhibit movement of the entire IIS4 segment, including the potential gating charges carried by R856 and K859, and it may further impede the movement of gating charges in other S4 segments through the allosteric interactions among voltage sensors described previously (Chanda et al., 2004). Third, the loss of depolarization-dependent reversal of block by ProTx-II also requires R850 and R853. These results suggest that R850 and R853 interact either sterically or electrostatically with ProTx-II as they move outward during activation and thereby push the toxin off its receptor site. Altogether, these three lines of evidence provide strong support for the conclusion that ProTx-II inhibits sodium channels by inhibiting the normal activation of the voltage sensor in domain II.

ProTx-II and β-scorpion toxins both affect sodium channel activation but have opposing effects on that process. According to our hypothesis, ProTx-II impedes gating charge movement and channel activation by trapping the IIS4 voltage sensor in its resting conformation. β-scorpion

Molecular Pharmacology Fast Forward. Published on December 21, 2007 as DOI: 10.1124/mol.107.041046
This article has not been copyedited and formatted. The final version may differ from this version.

toxins facilitate channel activation by trapping the IIS4 voltage sensor in its activated conformation. The specific effects of both β-scorpion toxin and ProTx-II on the IIS4 voltage sensor suggest that this voltage sensor may have a privileged role in the actions of gating modifier toxins that affect sodium channel activation, whether they enhance or inhibit it. Further studies are required to completely map the amino acid residues that form the receptor site for ProTx-II on $Na_V1.2$ channels.

In a recent study of site-directed mutants of $Na_V1.5$ channels, Smith et al. (2007) analyzed a large number of amino acid residues for involvement in the action of ProTx-II and found no major effects. They did not analyze the equivalent of mutant L833C, but they found that different mutations of residues in the IIS3-S4 loop had no effect on ProTx-II action in agreement with our work. Based on this extensive analysis, it appears that ProTx-II has a unique site of action compared to other gating modifier toxins. It will be of great interest to define its receptor site and determine how it impedes movement of the IIS4 voltage sensor.

Subtype-specific reversal of ProTx-II action. Brain and cardiac Na^+ channels display similar sensitivity for inhibition of channel activation by ProTx-II at hyperpolarized potentials where the channels are in their resting conformations (Fig. 1; see also Middleton et al., 2002). However, the rates for voltage-dependent reversal of protoxin-II inhibition differ substantially between $Na_v1.2$ and $Na_v1.5$. The cardiac $Na_v1.5$ isoform has faster and more prominent relief of inhibition at conditioning potentials ranging from +40 mV to +100 mV. These results indicate that at least part of the ProTx-II receptor site differs between brain and cardiac sodium channels and that the release of ProTx-II after voltage-dependent activation is more rapid for the $Na_v1.5$ channel. This suggests that ProTx-II has a lower affinity for the activated state of the $Na_v1.5$ channel than for that of $Na_v1.2$. Determination of the amino acid residues responsible for the difference in ProTx-II action between $Na_V1.2$ and $Na_V1.5$ channels may give insight into the molecular basis for the substantially different voltage dependence of activation of these channel subtypes.

Molecular Pharmacology Fast Forward. Published on December 21, 2007 as DOI: 10.1124/mol.107.041046
This article has not been copyedited and formatted. The final version may differ from this version.

Comparison of voltage-sensor trapping by ProTx-II and Hanatoxin. Hanatoxin is another gating modifier toxin that inhibits $K_V2.1$ channels (Swartz and MacKinnon, 1995). This channel is composed of 4 independent, identical subunits that form a noncovalently associated tetramer, in contrast to sodium channels whose four nonidentical, but homologous, domains are covalently linked in a single polypeptide chain. Hanatoxin blocks gating charge movement more completely than ProTx-II (Lee et al., 2003), as expected since hanatoxin binds to all four subunits of $K_V2.1$ channels and prevents gating movement of all four S4 segments. Like Protoxin-II, hanatoxin binding to only one of the four homologous subunits/domains is sufficient to impair channel opening (Swartz and MacKinnon, 1997; Lee et al., 2003), and hanatoxin affinity for $K_V2.1$ is reduced after prolonged depolarization (Phillips et al., 2005). Hanatoxin-blocked channels can open during long depolarizing pulses with toxin bound, resulting in accelerated deactivation (Swartz and MacKinnon, 1997) and also in strongly shifted voltage dependence of activation (Swartz and MacKinnon, 1997) that resembles the strong positive shift of the voltage dependence of activation observed for ProTx-II-blocked sodium channels (Fig. 5). Thus, hanatoxin and ProTx-II have similar mechanisms of action that depend on trapping a voltage sensor in its resting conformation. Differences in the details of their mechanisms of action likely reflect the ability of $K_V2.1$ channels to bind four hanatoxin molecules to their four voltage sensor domains.

Molecular Pharmacology Fast Forward. Published on December 21, 2007 as DOI: 10.1124/mol.107.041046
This article has not been copyedited and formatted. The final version may differ from this version.

References

Armstrong CM (1981) Sodium channels and gating currents. *Physiol Rev* **61:**644-682.

Auld VJ, Goldin AL, Krafte DS, Catterall WA, Lester HA, Davidson N, and Dunn RJ (1990) A neutral amino acid change in segment IIS4 dramatically alters the gating properties of the voltage-dependent sodium channel. *Proc Natl Acad Sci USA* **87:**323-327.

Benzinger GR, Kyle JW, Blumenthal KM, and Hanck DA (1998) A specific interaction between the cardiac sodium channel and site-3 toxin anthopleurin B. *J Biol Chem* **273:**80-84.

Cahalan MD (1975) Modification of sodium channel gating in frog myelinated nerve fibres by Centruroides sculpturatus scorpion venom. *J Physiol* **244:**511-534.

Catterall WA (1977) Membrane potential-dependent binding of scorpion toxin to the action potential Na^+ ionophore. Studies with a toxin derivative prepared by lactoperoxidase-catalyzed iodination. *J Biol Chem* **252:**8660-8668.

Catterall WA (1979) Binding of scorpion toxin to receptor sites associated with sodium channels in frog muscle. Correlation of voltage-dependent binding with activation. *J Gen Physiol* **74:**375-391.

Catterall WA (1980) Neurotoxins that act on voltage-sensitive sodium channels in excitable membranes. *Annu Rev Pharmacol Toxicol* **20:**15-43.

Catterall WA (1986) Molecular properties of voltage-sensitive sodium channels. *Annu Rev Biochem* **55:**953-985.

Catterall WA (2000) From ionic currents to molecular mechanisms: The structure and function of voltage-gated sodium channels. *Neuron* **26:**13-25.

Catterall WA and Beress L (1978) Sea anemone toxin and scorpion toxin share a common receptor site associated with the action potential sodium ionophore. *J Biol Chem* **253:**7393-7396.

Cestèle S and Catterall WA (2000) Molecular mechanisms of neurotoxin action on voltage-gated sodium channels. *Biochimie* **82:**883-892.

Cestèle S, Scheuer T, Mantegazza M, Rochat H, and Catterall WA (2001) Neutralization of gating charges in domain II of the sodium channel α subunit enhances voltage sensor trapping by β-scorpion toxins. *J Gen Physiol* **118:**291-302.

Cestèle S, Yarov-Yarovoy V, Qu Y, Sampieri F, Scheuer T, and Catterall WA (2006) Structure and function of the voltage sensor of sodium channels probed by a beta-scorpion toxin. *J Biol Chem* **281:**21332-21344.

Chanda B, Asamoah OK, and Bezanilla F (2004) Coupling interactions between voltage sensors of the sodium channel as revealed by site-specific measurements. *J Gen Physiol* **123:**217-230.

Chanda B and Bezanilla F (2002) Tracking voltage-dependent conformational changes in skeletal muscle sodium channel during activation. *J Gen Physiol* **120:**629-645.

Guy HR and Seetharamulu P (1986) Molecular model of the action potential sodium channel. *Proc Natl Acad Sci U S A* **508:**508-512.

Jaimovich E, Ildefonse M, Barhanin J, Rougier O, and Lazdunski M (1982) *Centruroides* toxin, a selective blocker of surface Na^+ channels in skeletal muscle: voltage-clamp analysis and biochemical characterization of the receptor. *Proc Natl Acad Sci U S A* **79:**3896-3900.

Jover E, Couraud F, and Rochat F (1980) Two types of scorpion neurotoxins characterized by their binding to two separate receptor sites on rat brain synaptosomes. *Biochem Biophys Res Commun* **95:**1697-1714.

Lee HC, Wang JM, and Swartz KJ (2003) Interaction between extracellular Hanatoxin and the resting conformation of the voltage-sensor paddle in Kv channels. *Neuron* **40:**527-536.

McPhee JC, Ragsdale DS, Scheuer T, and Catterall WA (1995) A critical role for transmembrane segment IVS6 of the sodium channel α subunit in fast inactivation. *J Biol Chem* **270:**12025-12034.

Meves H, Rubly N, and Watt DD (1982) Effect of toxins isolated from the venom of the scorpion Centruroides sculpturatus on the Na currents of the node of Ranvier. *Pflugers Arch* **393:**56-62.

Middleton RE, Warren VA, Kraus RL, Hwang JC, Liu CJ, Dai G, Brochu RM, Kohler MG, Gao YD, Garsky VM, Bogusky MJ, Mehl JT, Cohen CJ, and Smith MM (2002) Two tarantula peptides inhibit activation of multiple sodium channels. *Biochemistry* **41:**14734-14747.

Nicholson GM, Willow M, Howden MEH, and Narahashi T (1994) Modification of sodium channel gating and kinetics by versutoxin from the Australian funnel-web spider Hadronyche versuta. *Pflugers Arch* **428:**400-409.

Nonner W (1979) Effects of Leiurus scorpion venom on the "gating" current in myelinated nerve. *Adv Cytopharmacol* **3:**345-352.

Norton RS and Pallaghy PK (1998) The cystine knot structure of ion channel toxins and related polypeptides. *Toxicon* **36:**1573-1583.

Phillips LR, Milescu M, Li-Smerin Y, Mindell JA, Kim JI, and Swartz KJ (2005) Voltage-sensor activation with a tarantula toxin as cargo. *Nature* **436:**857-860.

Priest BT, Blumenthal KM, Smith JJ, Warren VA, and Smith MM (2007) ProTx-I and ProTx-II: gating modifiers of voltage-gated sodium channels. *Toxicon* **49:**194-201.

Rogers JC, Qu Y, Tanada TN, Scheuer T, and Catterall WA (1996) Molecular determinants of high affinity binding of α-scorpion toxin and sea anemone toxin in the S3-S4 extracellular loop in domain IV of the Na^+ channel α subunit. *J Biol Chem* **271:**15950-15962.

Sheets MF, Kyle JW, Kallen RG, and Hanck DA (1999) The Na channel voltage sensor associated with inactivation is localized to the external charged residues of domain IV, S4. *Biophys J* **77:**747-757.

Smith JJ, Cummins TR, Alphy S, and Blumenthal KM (2007) Molecular interactions of the gating modifier toxin ProTx-II with $Na_V1.5$: implied existence of a novel toxin binding site coupled to activation. *J Biol Chem* **282:**12687-12697.

Sokolov S, Scheuer T, and Catterall WA (2005) Ion permeation through a voltage- sensitive gating pore in brain sodium channels having voltage sensor mutations. *Neuron* **47:**183-189.

Stefani E and Bezanilla F (1998) Cut-open oocyte voltage-clamp technique. *Methods Enzymol* **293:**300-318.

Stuhmer W, Conti F, Suzuki H, Wang X, Noda M, Yahadi N, Kubo H, and Numa S (1989) Structural parts involved in activation and inactivation of the sodium channel. *Nature* **339:**597-603.

Swartz KJ and MacKinnon R (1995) An inhibitor of the Kv2.1 potassium channel isolated from the venom of a Chilean tarantula. *Neuron* **15:**941-949.

Swartz KJ and MacKinnon R (1997) Hanatoxin modifies the gating of a voltage-dependent K^+ channel through multiple binding sites. *Neuron* **18:**665-673.

Tejedor FJ and Catterall WA (1988) A site of covalent attachment of α-scorpion toxin derivatives in domain I of the sodium channel α subunit. *Proc Natl Acad Sci U S A* **85:**8742-8746.

Thomsen WJ and Catterall WA (1989) Localization of the receptor site for α-scorpion toxins by antibody mapping: implications for sodium channel topology. *Proc Natl Acad Sci U S A* **86:**10161-10165.

Yang N and Horn R (1995) Evidence for voltage-dependent S4 movement in sodium channel. *Neuron* **15:**213-218.

Yarov-Yarovoy V, Baker D, and Catterall WA (2006) Voltage sensor conformations in the open and closed states in ROSETTA structural models of K^+ channels. *Proc Natl Acad Sci U S A* **103:**7292-7297.

Molecular Pharmacology Fast Forward. Published on December 21, 2007 as DOI: 10.1124/mol.107.041046
This article has not been copyedited and formatted. The final version may differ from this version.

Figure Legends

Fig. 1. Effects of ProTx-II on properties of ionic currents through $Na_v1.2a$ α subunits coexpressed with β1 subunits in Xenopus oocytes. A, C, Currents were elicited using 10 ms depolarizations to potentials from -60 mV to +75 mV in 5 mV steps from a holding potential of -100 mV. A, Families of ionic currents before (top) and 5 min after bath application of 1 μM ProTx-II (bottom). For potentials between -60 to -20 mV, traces are shown every 5 mV. At more positive potentials the interval is 10 mV. B, Concentration-response relationship for ProTx-II block of sodium current at -10 mV. The data were fit with a one-site binding isotherm with an EC_{50} of 540 nM ($n \geq 3$ for each concentration). C, Normalized conductance-voltage relationship for $Na_v1.2a/\beta1$ channel before (squares, $V_{1/2}$= -26.7 mV, k=5.9 mV, n=15) and after application of 1 μM ProTx-II (open circles, $V_{1/2}$= -25.7 mV, k=6.9 mV, Normalized G_{max}=0.36±0.03, n=12). Error bars are smaller than the symbols. D, Voltage dependence of the time constant of current decay (τ) during the 10 ms depolarizations to the indicated potentials for $Na_v1.2a/\beta_1$ in control (filled squares, n=14) and with 1 μM ProTx-II (open circles, n=12). E, Kinetics of recovery from fast inactivation induced by a 20 ms conditioning pulse to -10 mV in control (filled squares, τ=2.2±0.3 ms, n=5) and in the presence of 1 μM ProTx-II (open circles, τ=2.5±0.3 ms, n=7). A 5 ms test pulse to -10 mV was applied after a recovery interval of variable duration at the holding potential of -100 mV. Fractional recovery was measured as the peak inward current during this test pulse normalized to peak inward current during the conditioning pulse. F, Voltage dependence of steady-state inactivation in control (filled squares, $V_{1/2}$ = -48.8±0.3 mV, n=6) and with 1 μM ProTx-II (open circles, $V_{1/2}$= -47.4±0.4 mV, n=9). Conditioning pulses of 200 ms to the indicated potentials were followed by 5-ms test pulses to -10 mV.

Molecular Pharmacology Fast Forward. Published on December 21, 2007 as DOI: 10.1124/mol.107.041046
This article has not been copyedited and formatted. The final version may differ from this version.

Fig. 2. Inhibition gating currents of $Na_v1.2a$ channels by ProTx-II. A, Representative on- and off-gating currents Q_{on} and Q_{off} in control (left) and after addition of 1 μM ProTx-II to bath (right) were recorded in the presence of 1 μM TTX to block ionic currents through the central pore of $Na_v1.2a$. Depolarizations 10 ms long to potentials from -90 mV to +100 mV were applied from a holding potential of -100 mV. For this representative experiment, gating charge was reduced by 27% at +100 mV. B, Mean normalized voltage dependence of Q_{on} gating charge movement in control (squares, n=7) and 5 min after application of 1 μM ProTx-II (open circles, n=5). Gating currents for each experiment were normalized to Q_{on} at +50 mV in the absence of toxin. C, Mean values for percent block by 1 μM ProTx-II of ionic current (at –10 mV, 65.3±4.1%, n=13) and gating charge Q_{on} (at +100 mV, 24.6 ± 6.8%, n=5).

Fig. 3. Selective inhibition of a fast component of gating charge Q_{on} by ProTx-II. A, Kinetics of Q_{on} movement showed in expanded scale in response to a depolarization to +50 mV from a holding potential of –100 mV in control (CON) and with 1 μM ProTx-II (PRO). B, Subtraction of gating charge movement kinetics without and with ProTx-II (shaded area) reveals that ProTx-II blocks only the fast component of gating charge Q_{on}. C, Fraction of ON gating current, I_{Qon}, blocked by ProTx-II as measured at the peak of I_{Qon} (Peak Q, n=10) or at a time when I_{Qon} in the absence of toxin had decayed to 20% of its peak value (Late Q) (n=9).

Fig. 4. Reversal of ProTx-II inhibition by strong depolarization. A, Pulse protocol for toxin reversal experiments includes a conditioning depolarization to +100 mV of varying duration ranging from 10 ms to 630 ms, a 20 ms return to the holding potential of –100 mV to allow recovery from fast inactivation, and a test pulse (-10 mV for ionic and +50 mV for gating

Molecular Pharmacology Fast Forward. Published on December 21, 2007 as DOI: 10.1124/mol.107.041046
This article has not been copyedited and formatted. The final version may differ from this version.

currents). B, Ionic (left) and gating (right) currents recorded in the presence of 1 μM ProTx-II increase in amplitude as the duration of the conditioning depolarization increases (arrows indicate current after the shortest (10 ms) conditioning pulse). C, Kinetics of ionic (circles, τ=0.39±0.08 s, n=4) and gating (squares, τ=0.36±0.06 s, n=4) current increase due to prolonged conditioning at +100 mV. To isolate the time course of voltage-dependent relief of toxin block of ionic and gating current, the data were normalized as follows. The steady-state level of ionic or gating current recorded during test pulses to -10 or +50 mV, respectively, in the presence of ProTx-II, were set to 0. The amount of current achieved after a 630 ms long depolarization to +100 mV was set to 1. Normalized I as a function of time (t) was plotted as [I(t)-I(0)]/[(I(630 ms)-I(0)].

Fig. 5. Voltage dependence of reversal of protoxin-II inhibition. A, Pulse protocol for estimation of voltage dependent kinetics of reversal of toxin inhibition of ionic current. Conditioning pulses of increasing duration (10 ms to 630 ms) were applied at various amplitudes (+40 mV to +100 mV) followed by a 20 ms repolarization to the holding potential of -100 mV and test pulse to -10 mV. Representative test pulse traces of ionic current recorded after conditioning pulses of 10, 30, 50, 90, 170, 310 and 630 ms to the indicated potentials are shown. Arrows denote ionic current after the 10 ms conditioning pulse. B, Voltage dependence of reversal at +100 mV (circles, τ=0.39±0.08s, n=5), +80 mV (triangles, τ=0.89±0.23 s, n=4), +60 mV (inverted triangles, τ=1.13±0.13s, n=4) and +40 mV (squares, τ=1.5±0.1 s, n=4). Peak test pulse ionic current ($I_{test\ pulse\ n}$)was measured and normalized to that recorded after the 10 ms ($I_{test\ pulse\ 1}$) conditioning depolarization. Normalized current [100*($I_{test\ pulse\ n}$)/ ($I_{test\ pulse\ 1}$)] is plotted versus conditioning pulse duration. C, Voltage dependence of activation of toxin-modified channels. Peak test pulse

Molecular Pharmacology Fast Forward. Published on December 21, 2007 as DOI: 10.1124/mol.107.041046
This article has not been copyedited and formatted. The final version may differ from this version.

currents after 630 ms prepulses to various potentials from experiments in B were measured and normalized to the peak test pulse current achieved at the most positive potential (150 mV). These normalized test pulse currents following 630 ms prepulses to the indicated potentials are plotted as a function of prepulse potential (open squares) and fit with a Boltzmann relationship with V_{half}= 64 mV and k = 17.4 mV. The normalized activation curve for control peak sodium current from Fig. 1B is replotted for comparison (filled circles).

Fig. 6. Voltage-dependent kinetics of reversal of ProTx-II inhibition for $Na_v1.2a$ and $Na_v1.5$ channels. A, Currents through $Na_v1.2a/\beta_1$ and $Na_v1.5/\beta_1$ channels before (CON) and 5 min after application of 1 μM ProTx-II to the external solution (PRO). B, Normalized kinetics of toxin reversal due to +100 mV conditioning depolarization for representative cells expressing either $Na_v1.2a$ (circles) or $Na_v1.5$ (open squares). Same pulse protocol as in Fig. 5 was used. C, The voltage dependent kinetics of ProTx-II reversal by conditioning depolarization for $Na_V1.2a$ (black bars, n≥5) and $Na_V1.5$ (white bars, n≥5).

Fig. 7. Effects of point mutations in the IIS3-S4 linker on inhibition by protoxin-II. A, A wash-in assay was used to estimate sensitivity of mutant channels to ProTx-II. Central pore current was recorded at during test pulses to –10 mV applied every 10 s in control conditions (CON) and for 3 min once 1 μM ProTx-II have been added to recording chamber. Percentage of peak current inhibition by the end of 3 min period is taken as a measure of toxin sensitivity. Representative currents for the wild type $Na_v1.2a$ (left) and mutant L833C channel (right) are shown. B, Percentage of peak current inhibited by 1 μM ProTx-II for wild type and various point mutants in the IIS3-S4 linker (n≥4). The inset indicates the amino acid sequence of $Na_V1.2a$ between amino acids 831 to 860 with the mutated amino acids indicated in bold.

Molecular Pharmacology Fast Forward. Published on December 21, 2007 as DOI: 10.1124/mol.107.041046
This article has not been copyedited and formatted. The final version may differ from this version.

Fig. 8. Altered effects of ProTx-II on ionic and gating current for mutant RR850,853QQ. A, Wash-in of 1.25 μM ProTx-II in wild type $Na_v1.2a$ (left) and mutant channel (right). Arrows denote current amplitude 3 min after addition of toxin to the bath. B, Loss of effect of ProTx-II on gating current in RR850,853QQ channels. *Left,* Gating current transients during depolarizations to +100 mV for WT and RR850,853QQ channels in the absence (CON) and presence (PRO) of ProTx-II. Right, Mean block of peak gating current at +100 mV by 1.25 μM ProTx-II in WT and RR850,853QQ channels ($n \geq 3$). C, Pulse protocol for conditioning-dependent toxin reversal and representative records in the presence of 1.25 μM ProTx-II for $Na_v1.2a$ and RR850,853QQ. Arrows denote current in the absence of conditioning. The slight decrease in current in RR850,853QQ is mainly due to slow inactivation of channels during conditioning pulses. D, Kinetics of conditioning-dependent current relief normalized to the current in the absence of conditioning for $Na_v1.2a$ (control, open circles, n=4; 1.25 μM ProTx-II, filled circles, n=5) and RR850,853QQ (control, open squares, n=6; 1.25 μM ProTx-II, filled squares, n=6).

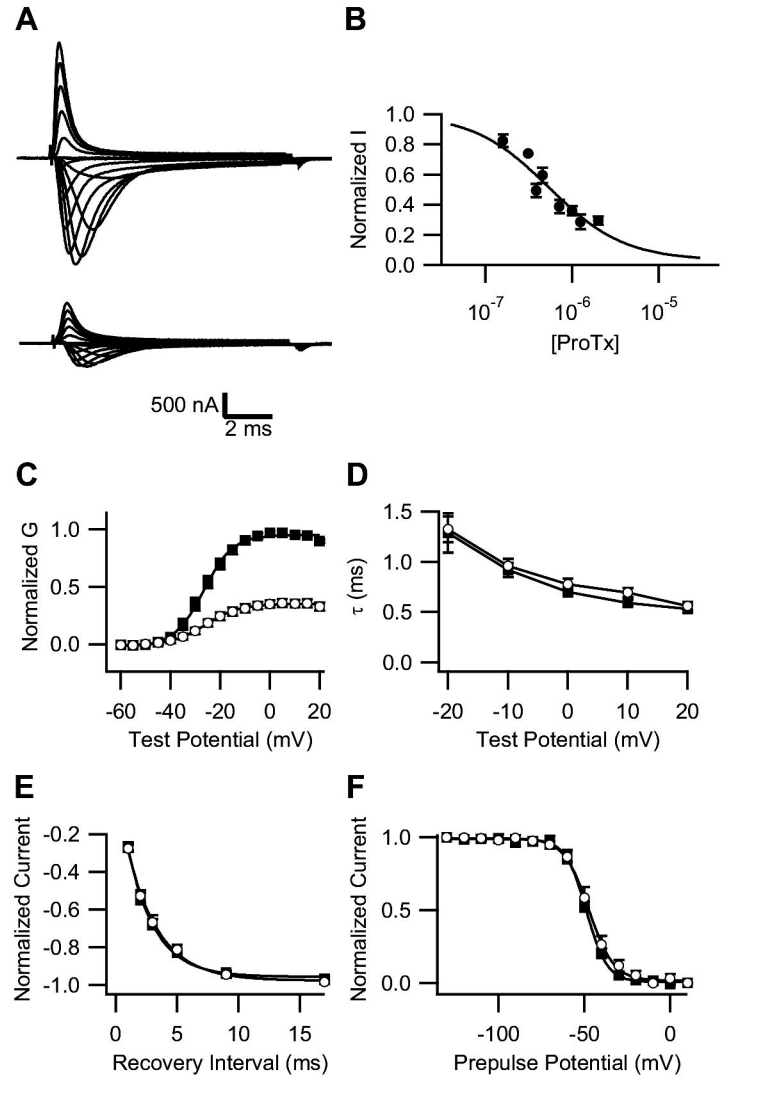
A
B
Normalized I
1.0
0.8
0.6
0.4
0.2
0.0
10^{-7}
10^{-6}
10^{-5}
[ProTx]
500 nA
2 ms
C
D
Normalized G
1.0
0.5
0.0
-60 -40 -20 0 20
Test Potential (mV)
τ (ms)
1.5
1.0
0.5
0.0
-20 -10 0 10 20
Test Potential (mV)
E
F
Normalized Current
-0.2
-0.4
-0.6
-0.8
-1.0
0 5 10 15
Recovery Interval (ms)
Normalized Current
1.0
0.5
0.0
-100 -50 0
Prepulse Potential (mV)

Figure 1

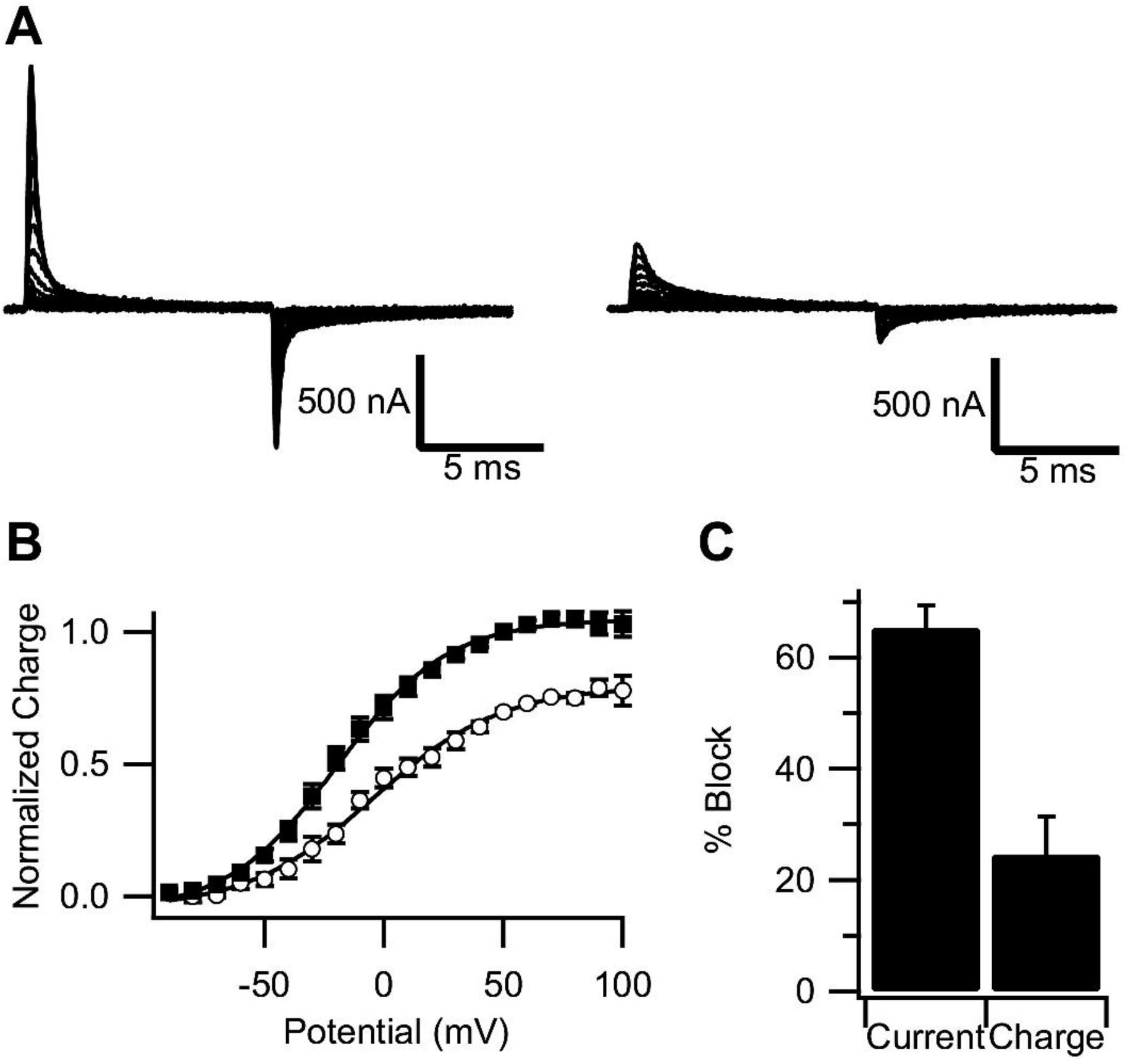
A
500 nA
5 ms
500 nA
5 ms
B
Normalized Charge
1.0
0.5
0.0
-50
0
50
100
Potential (mV)
C
% Block
60
40
20
0
Current
Charge

Figure 2

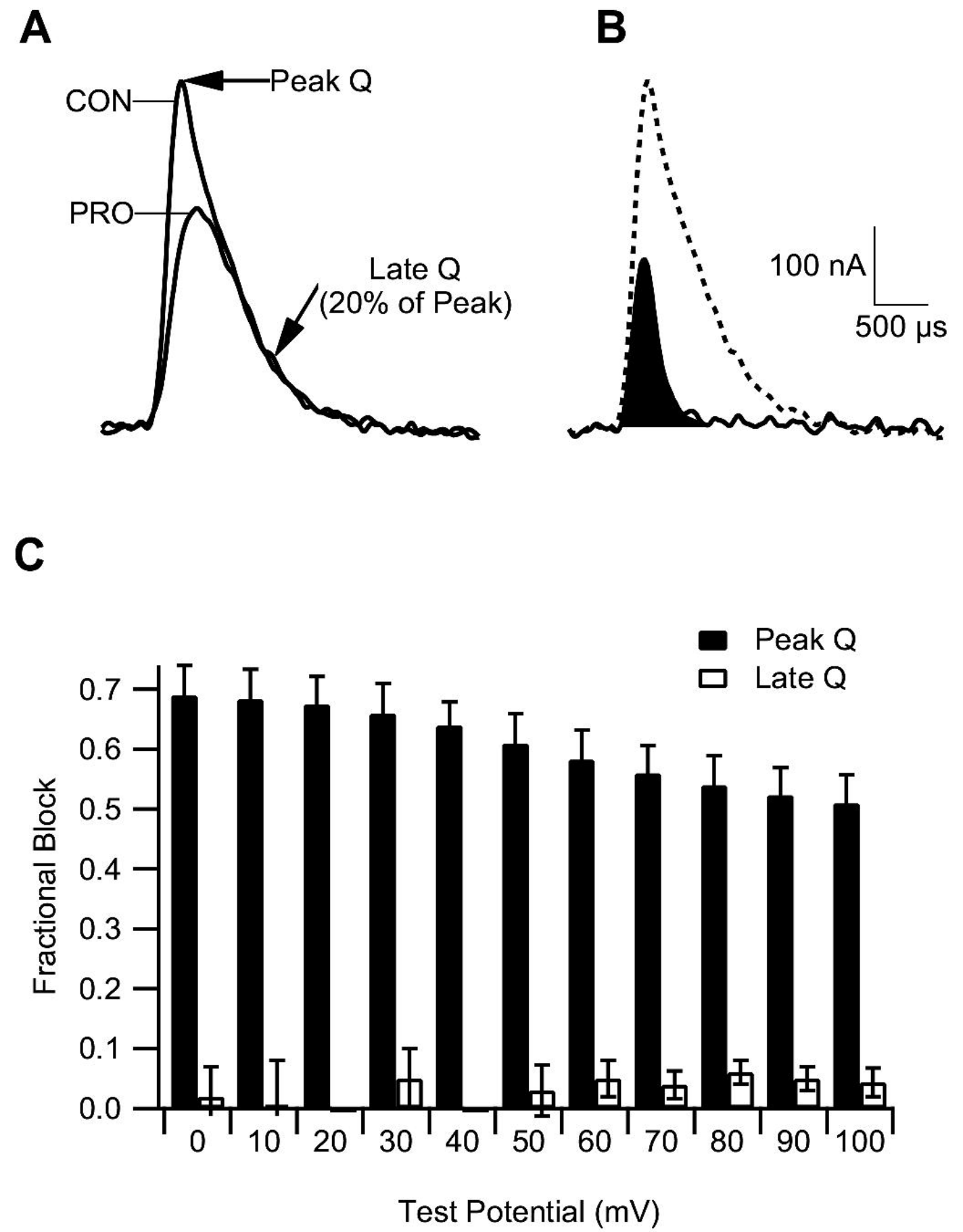
A
CON
Peak Q
PRO
Late Q
(20% of Peak)
B
100 nA
500 µs
C
Peak Q
Late Q
Fractional Block
0.0
0.1
0.2
0.3
0.4
0.5
0.6
0.7
0
10
20
30
40
50
60
70
80
90
100
Test Potential (mV)

Figure 3

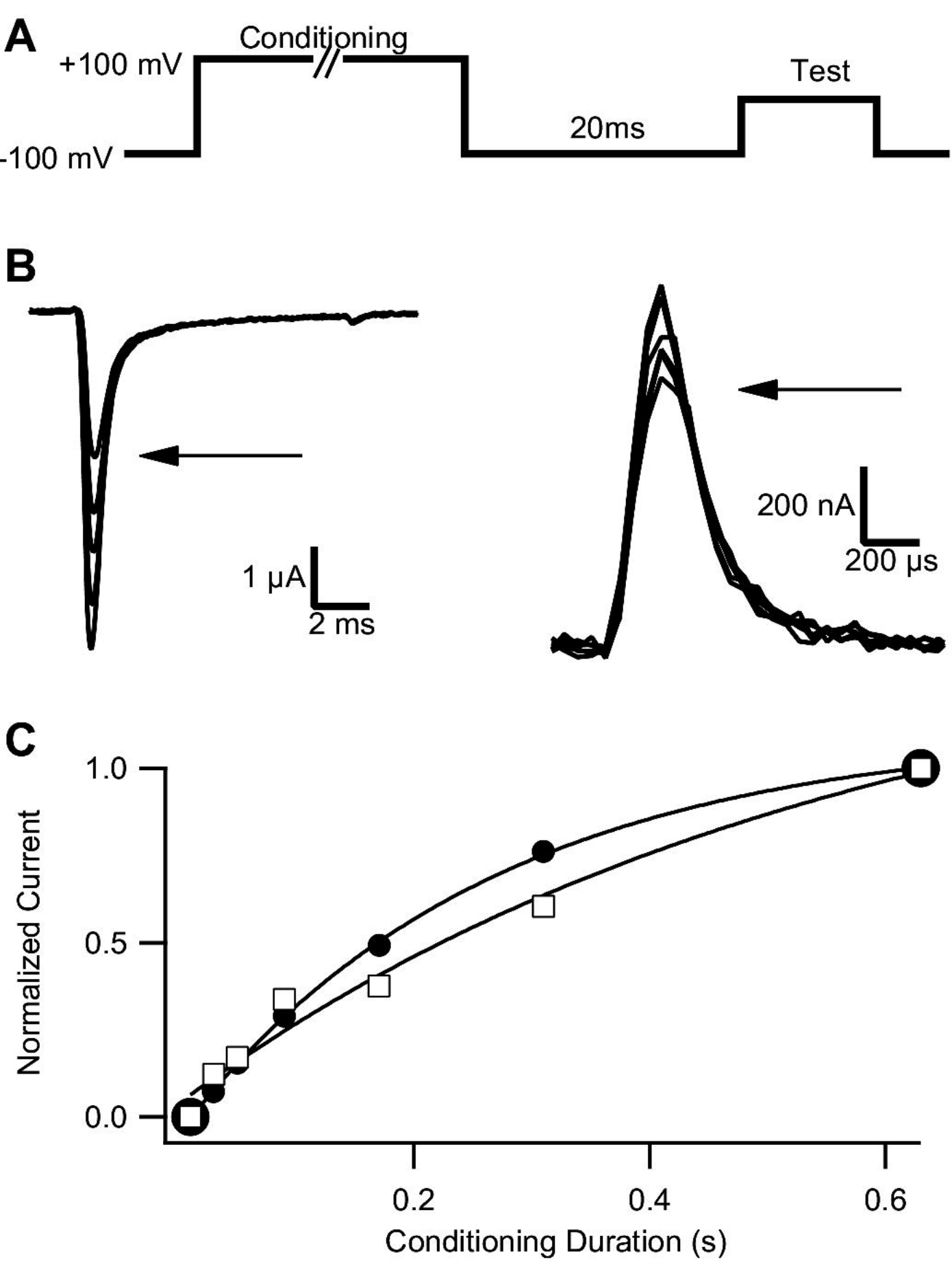
A
+100 mV
Conditioning
Test
20ms
-100 mV
B
1 µA
2 ms
200 nA
200 µs
C
Normalized Current
1.0
0.5
0.0
0.2
0.4
0.6
Conditioning Duration (s)

Figure 4

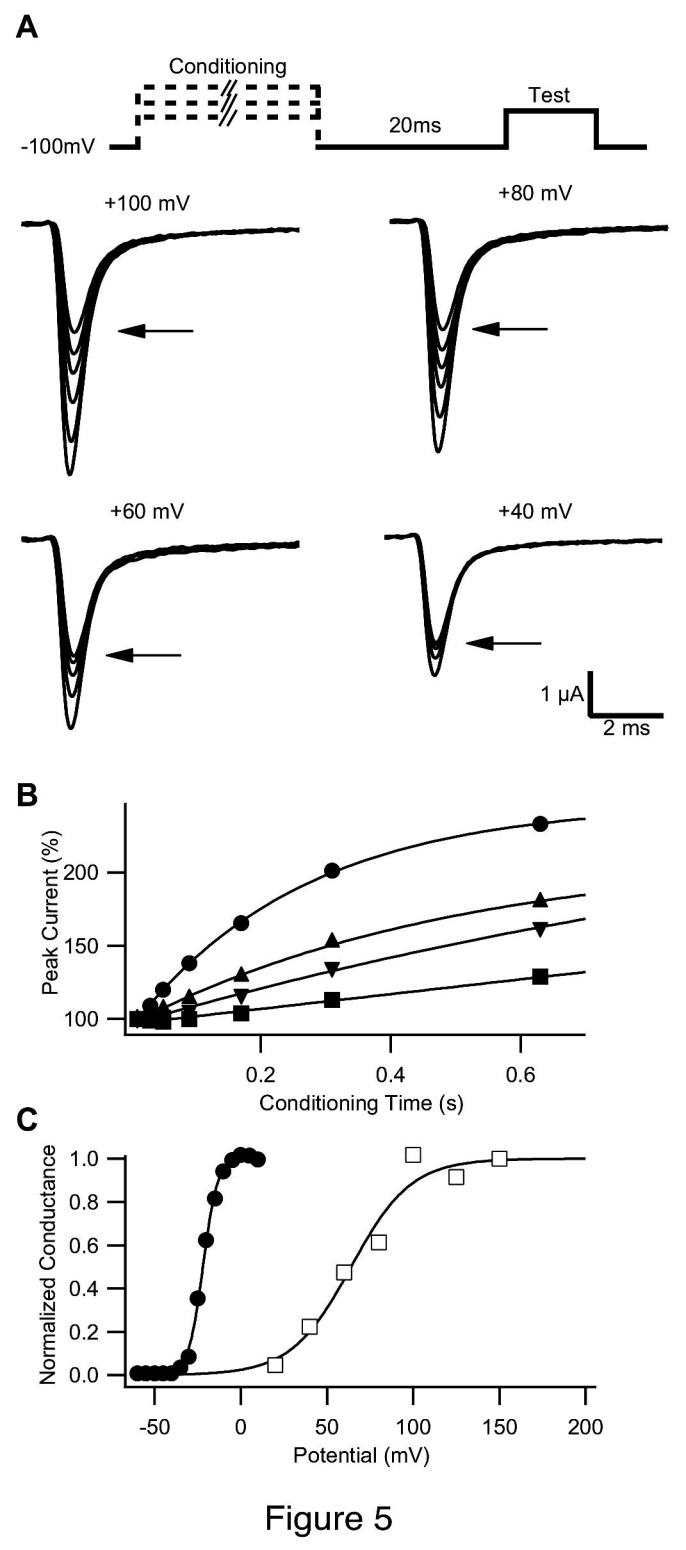
A
Conditioning
Test
-100mV
20ms
+100 mV
+80 mV
+60 mV
+40 mV
1 µA
2 ms
B
Peak Current (%)
200
150
100
0.2
0.4
0.6
Conditioning Time (s)
C
Normalized Conductance
1.0
0.8
0.6
0.4
0.2
0.0
-50
0
50
100
150
200
Potential (mV)

Figure 5

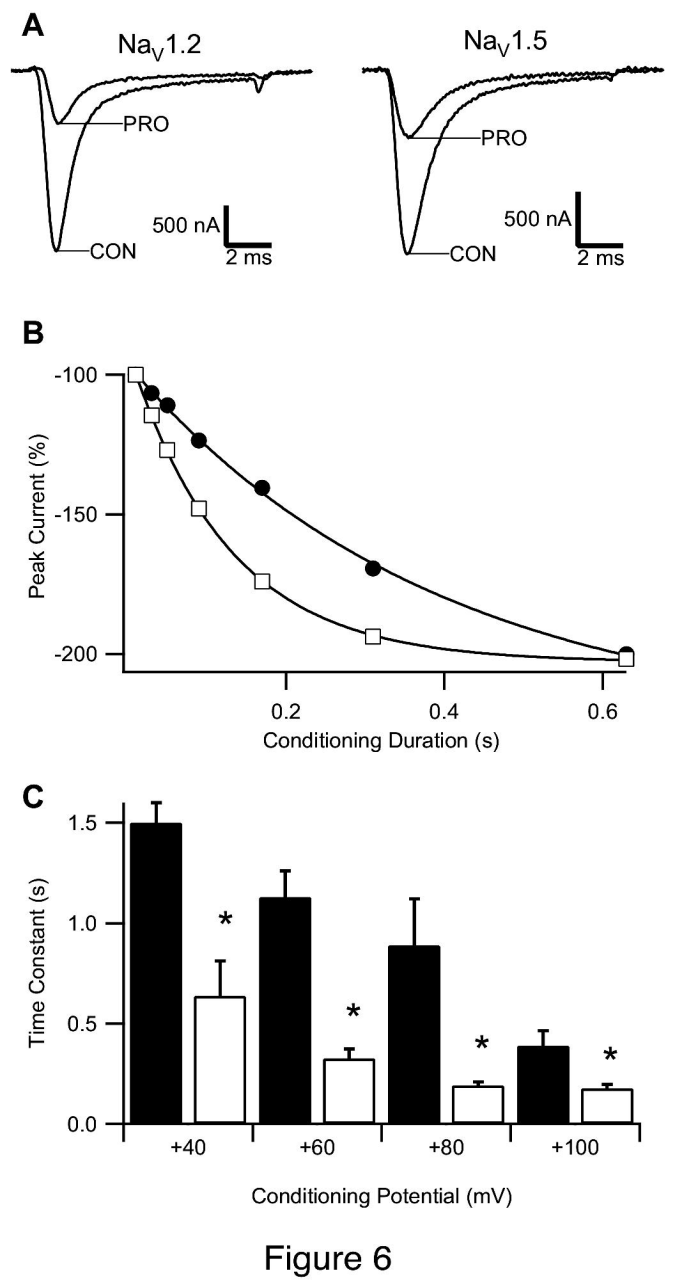
A
Na$_V$1.2
PRO
CON
500 nA
2 ms
Na$_V$1.5
PRO
CON
500 nA
2 ms
B
-100
-150
-200
Peak Current (%)
0.2
0.4
0.6
Conditioning Duration (s)
C
1.5
1.0
0.5
0.0
Time Constant (s)
*
*
*
*
+40
+60
+80
+100
Conditioning Potential (mV)

Figure 6

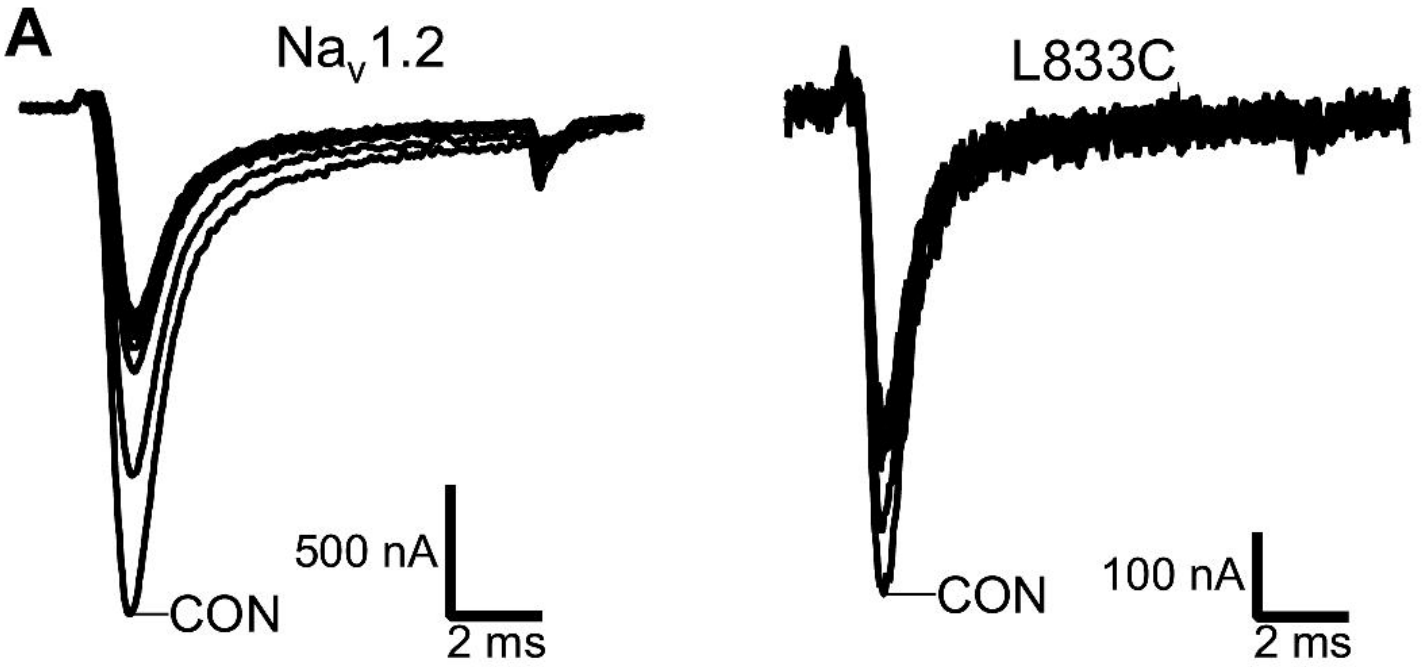
A
Na$_v$1.2
CON
500 nA
2 ms
L833C
CON
100 nA
2 ms

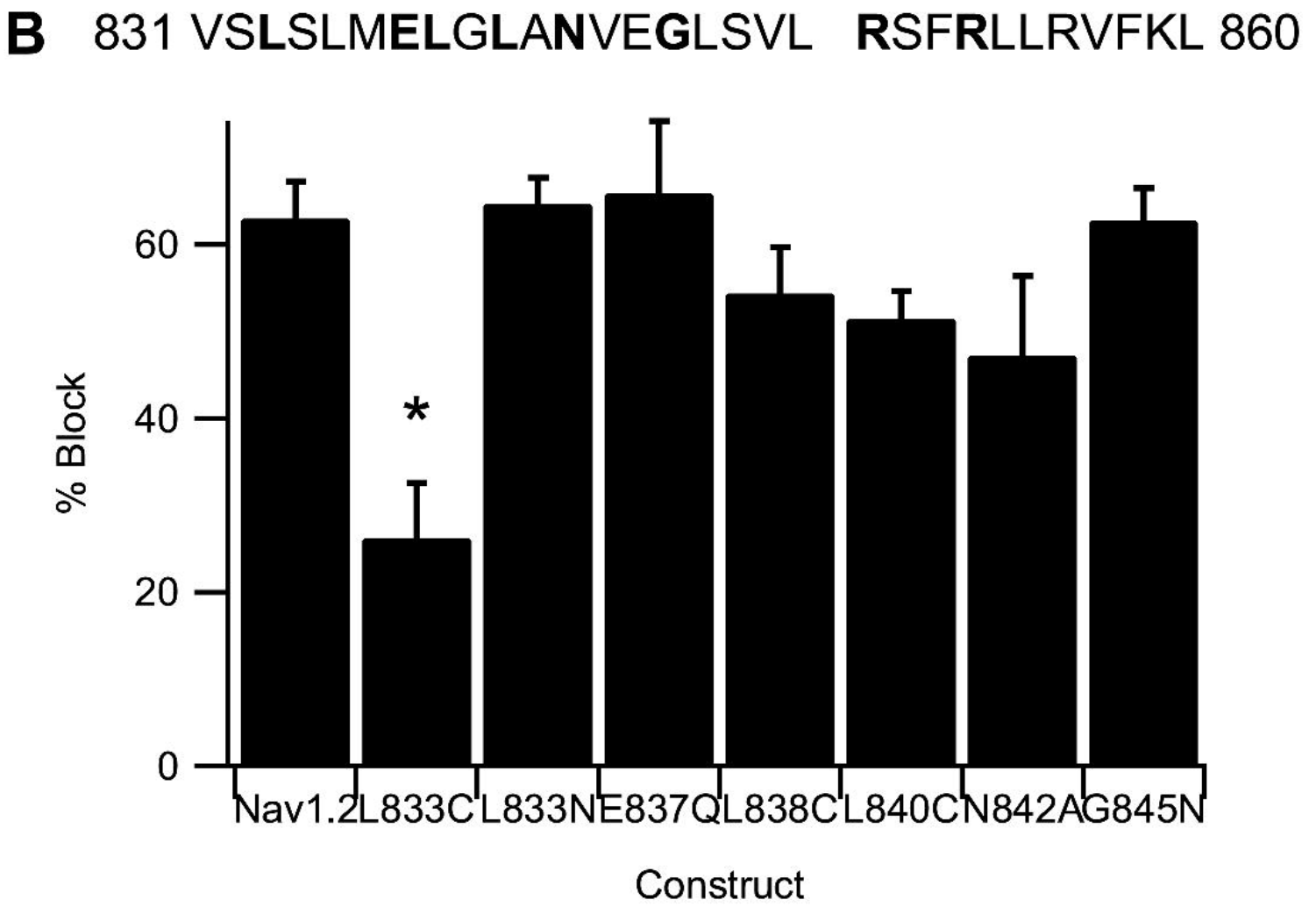
B 831 VSLSLMELGLANVEGLSVL RSFRLLRVFKL 860
% Block
0
20
40
60
*
Nav1.2
L833C
L833N
E837Q
L838C
L840C
N842A
G845N
Construct

Figure 7

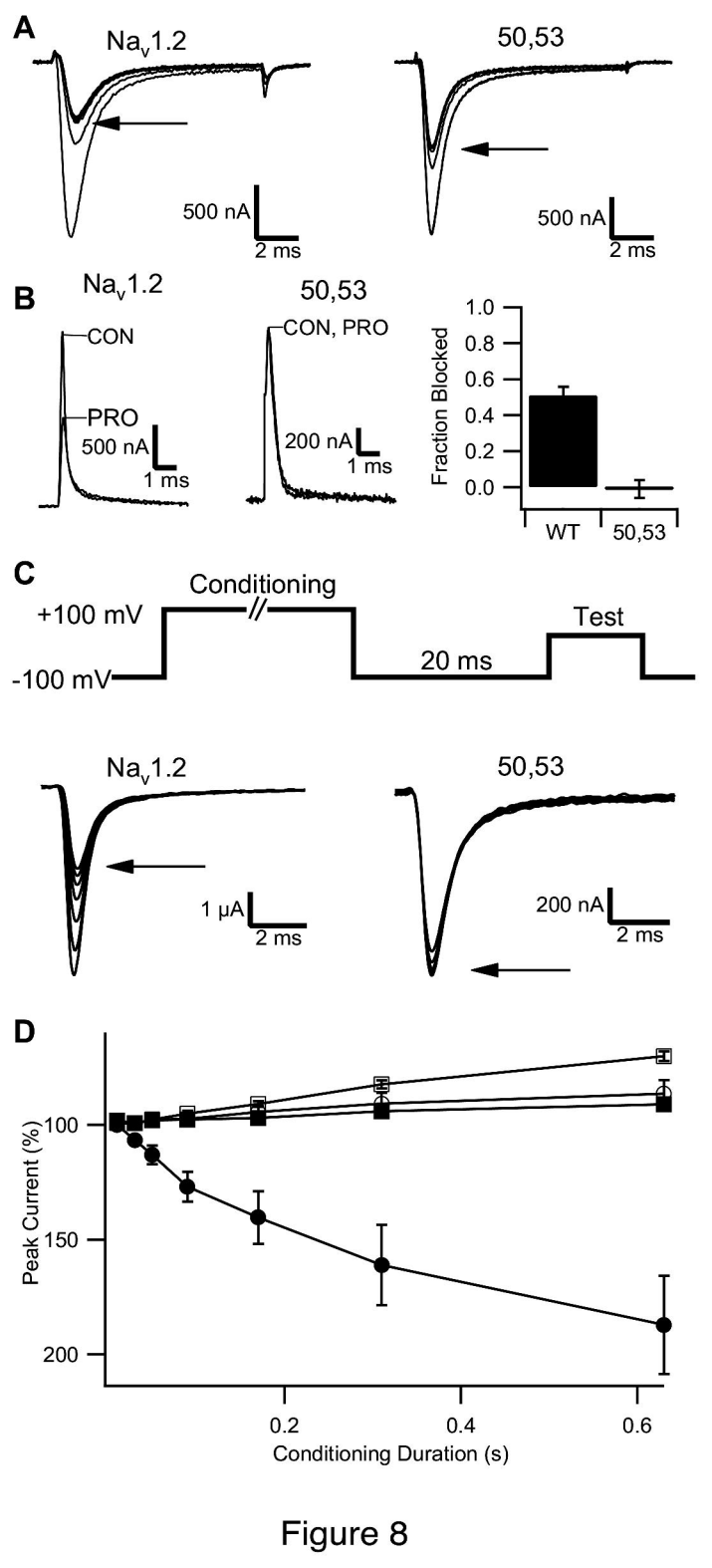
A
Na$_v$1.2
500 nA
2 ms
50,53
500 nA
2 ms
B
Na$_v$1.2
CON
PRO
500 nA
1 ms
50,53
CON, PRO
200 nA
1 ms
Fraction Blocked
1.0
0.8
0.6
0.4
0.2
0.0
WT
50,53
C
Conditioning
+100 mV
-100 mV
20 ms
Test
Na$_v$1.2
1 µA
2 ms
50,53
200 nA
2 ms
D
Peak Current (%)
100
150
200
0.2
0.4
0.6
Conditioning Duration (s)

Figure 8